Advances in Computational Design, *Vol. 10, No. 1 (2025) 73-89*
https://doi.org/10.12989/acd.2025.10.1.073

Design analysis and system identification of micro gripper with polymer smart actuator

Neeta Sahay*[1], Subrata Chattopadhyay[2] and Tamonash Jana[3]

[1]Department of Electrical and Electronics Engineering Institute of Engineering & Management, Kolkata, Sector V, Saltlake City, Kolkata-700091, West Bengal, India
[2]Department of Electrical Engineering National Institute of Technical Teachers' Training and Research, Kolkata, Block FC, Saltlake City, Kolkata-700106, West Bengal, India
[3]Department of Mechanical Engineering Institute of Engineering & Management, Kolkata, Sector V, Saltlake City, Kolkata-700091, West Bengal, India

(Received October 3, 2024, Revised November 7, 2024, Accepted February 4, 2025)

Abstract. This research paper presents design analysis of a microgripper made up of Thermo-plastic Polyurethane (TPU) material with smart actuation by Ionic Polymer Metal Composite (IPMC) for Micromanipulations. The microgripper has been designed by Pro Release 5.0 software using TPU as the base material which is of very flexible, light weight and low cost. IPMC has been used as the smart actuator which is an Electro active polymer (EAP) operated with low voltage application (1–5 V) for typical sample of dimension 40 mm × 10 mm × 0.2 mm. The gripper is able to provide gripping at its jaw due to deformation of the actuator inserted within it. Displacement analysis has been done using Finite element method (FEM) in ANSYS where the maximum displacement of the gripper jaw has been recorded to obtain the in-put-output characteristics of the structure which is found to be linear in the range of interest. The microgripper system modeling has been done using system identification toolbox in MATLAB where the estimated transfer function model is validated using MATLAB Simulink.

Keywords: displacement analysis; Ionic Polymer Metal Composite (IPMC); microgripper; pro release 5.0; simulink; smart actuation; system identification

1. Introduction

In the field of robotics, the complex process of fingers and gripper design has been evolved as an emerging field of research. The research devoted by (Al-Maliki *et al*. 2020) to analyze thermal and mechanical dynamic behavior of a beam reinforced with graphene platelets (GPLs) based on finite element approach. The formula presented is based on a higher order refined beam element accounting for shear deformations. (Ali *et al*. 2022) has analyzed a nonlinear bending behaviors of composite magneto-electro-elastic (MEE) nano-scale beams. The composite beam is assumed to be under a transverse mechanical load produced from piezoelectric and magnetic ingredients. In the paper described by (Polatov *et al*. 2020) the technology for constructing a finite element

*Corresponding author, Assistant Professor, E-mail: neetashy82@gmail.com

 ISSN: 2383-8477 (Print), 2466-0523 (Online)

representation of a multiply connected three-dimensional area has been proposed. The most useful rehabilitation methods used to reinforcement composite is to contribute to the rapid and effective repair of structures, as it can also restore to the load-bearing (Benhenni *et al*. 2018). (Daouadji *et al*. 2016) has shown an improved method for calculating interface stresses and the validation of the proposed model was carried out by comparison with those of the most recent results from the literature. The methodology developed by (Ertas *et al*. 2011, Kayikci *et al*. 2012) is to maximize the load-carrying capacity or strength of composite structures by minimizing the maximum stress where a global search algorithm called the direct search simulated annealing has been adopted to optimize the process. In the research paper (Pavarino *et al*. 2013), a process alternatives to solid modeling and automatic generation of highly refined tetrahedral meshes, with highly compatible with other studies focused on generation of mesh has been demonstrated. (Abderezak *et al*. 2021) presented an analysis and modeling of the concentrations of interfacial stresses in a damaged reinforced concrete beam strengthening in bending by an imperfect FGM plate based on a development of a mathematical formulation.

A miniaturized (MEMS)-based microgripper device system has been proposed sized ranging from 5 μm to 20 μm with a maximum applied force of 13.33 mN. The proposed microgripper with thermal actuator and capacitive force sensor has been designed using standard silicon-on-insulator multi-user MEMS processes with a device size of 2.5 × 3.2 mm^2 and analyzed by Finite element method (Tariq *et al*. 2022). The design of Ferromagnetic Shape Memory Alloy (FSMA) has been proposed by (Bagchi *et al*. 2021). The abricated FSMA microgripper was designed by a standard Computer Aided Engineering (CAE) software and numerical characterization was performed with Finite Element Analysis (FEA) by CAE software. Design and analysis of offshore wind structure has been carried out by (You at al. 2021). (Karpik *et al*. 2023) has presented a review where the reasons and advantages of increasing order elements demonstrated the providence of variants that are associated with reducing number of integration. (Mandal *et al*. 2017) has presented the performance of eight noded brick element by finite element method using MATLAB simulation giving good results in comparison to the standard linear method in terms of deflections at each nodal points. The foundation structure was created in the CAD construction software, Autodesk Inventor, and then imported into the FE software, ANSYS Workbench 19.0. Therefore, the Finite element model represents the optimum geometry. The paper presented by (Ramasubramanian *et al*. 2022), a simulation method has been developed for generating automatically new iterations of the gripper finger as well as to validate its performance. (Hassan *et al*. 2017) proposed a process for modeling and optimizing robot structure via case study where a robot gripper has a closed-loop mechanism with single degree of freedom (DOF) structure. (Yang *et al*. 2021), presented a novel three-degrees-of-freedom piezoelectric compliant microstage with double-rocker mechanism. An analytical model is proposed to evaluate the deformation characteristics of the microstage and the model is compared using finite-element analysis (FEA). (Vokoun *et al*. 2015), has considered the motion of an IPMC as a cantilever under a periodic voltage. The 3D model has been analyzed by finite element method considering both the free tip displacements and the blocking forces for various thicknesses and elastic constants of the ionomer membrane. In order to assess the effect of dehydration on bending resistance and bending response, (Biswal *et al*. 2014), has analyzed an IPMC actuator by variable parameters pseudo-rigid body modeling (VPPRBM) technique for various input voltages. (Gupta *et al*. 2022), explored the IPMC as soft actuator and actuation characteristics in underwater environment has been evaluated using data acquisition using LabView. Proportional, Integral and Derivative (PID) controller was adopted through MATLAB/ Simulink for better closed-loop response. (Zhao *et al*. 2020), designed a piezoelectric microgripper

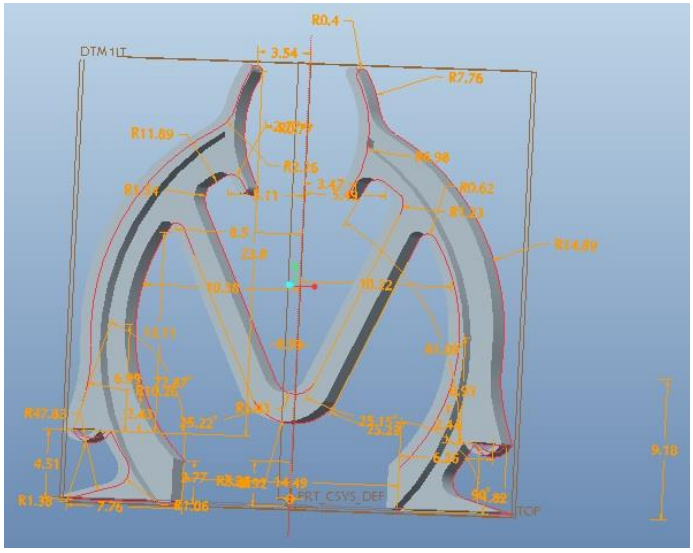

Fig. 1 3D modeling of Microgripper with driving dimensions (mm)

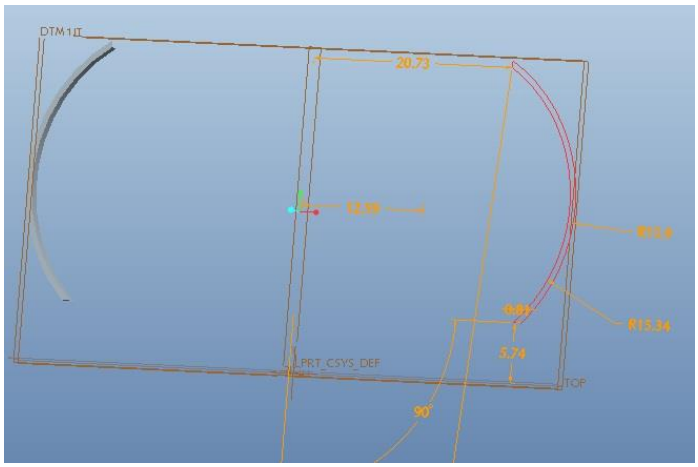

Fig. 2 3D design of actuator with driving dimensions (mm)

with three-stage amplification, which is able to produce the tip displacement and gripping force. The parameters of the microgripper were optimized by finite element method and compared with its theoretical amplification ratio. (Sun *et al*. 2014), investigated and verified the characteristics of IPMC actuators theoretically as well as experimentally. Combining static and dynamic models the transfer function of the IPMC actuator has been derived with respect to mechanical response to an electrical signal. (Shan *et al*. 2023), proposed a soft robotic gripper with multi-stem twining which can realize a larger contact area of surrounding preserving the advantages of twining grasping and increased grasping force.

In this research work the design of a robotic microgripper made up of Thermoplastic Polyurethane (TPU) materials is presented. The microgripper is operated by smart actuation using IPMC strip of required dimension. The microgripper has been designed with Pro Release 5.0

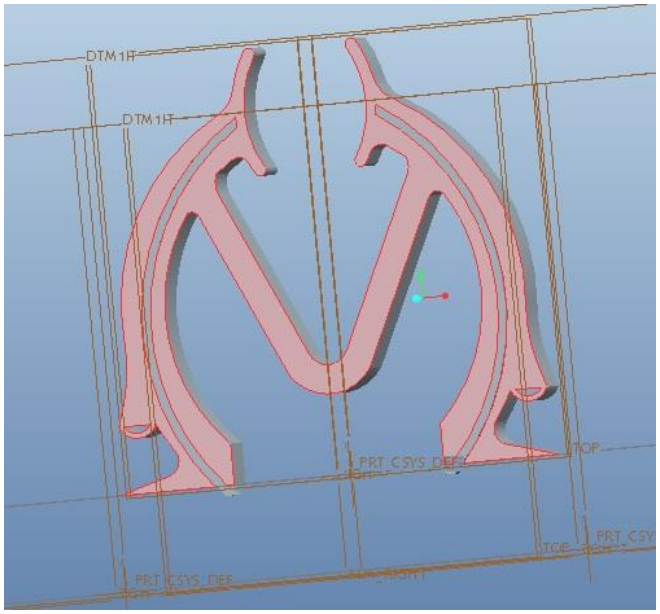

Fig. 3 3D modeling of TPU microgripper with IPMC actuator assembly

Table 1 Performance comparison of different prediction models

Properties	IPMC	TPU
Tensile Strength Yield	21 MPa	9 MPa
Density	3.385 g/cc	1.21 g/cc
Poissons's Ratio	0.4	0.36
Modulus of Elasticity	105 MPa	26 MPa

software and displacement analysis performed by ANSYS R18.2 considering displacements of the gripper jaw due to different static pressure generated along its length due to smart actuation of IPMC by electrical energy.

2. Design of microgripper with IPMC actuator

The microgripper is designed in normally open mode by Pro Release 5.0 as shown in Fig. 1 (the top viewed gripper with all major dimensions). In the Fig. 2, the design of the IPMC actuator has been presented which will be inserted within the gripper made up of TPU. Fig. 3, reveals the 3D view of the assembly structure, the TPU microgripper with IPMC actuator. In Table 1, mechanical properties of two governing materials, IPMC and TPU, has been presented.

3. Stress and displacement analysis of TPU microgripper with IPMC actuator

The gripper body is developed by TPU which is of very light weight and sufficiently flexible for micromanipulation. Fig. 4 shows the microgripper - actuator assembly with pressure applied

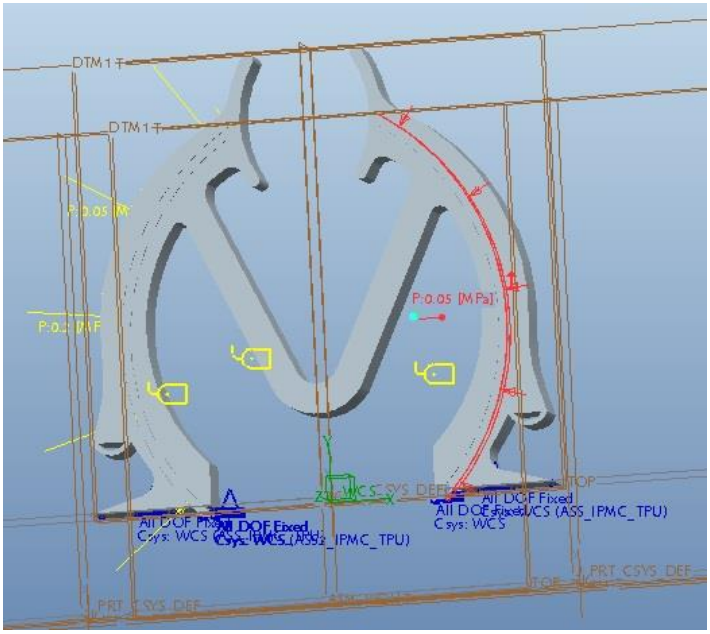

Fig. 4 3D view of the gripper assembly with area of application of pressure

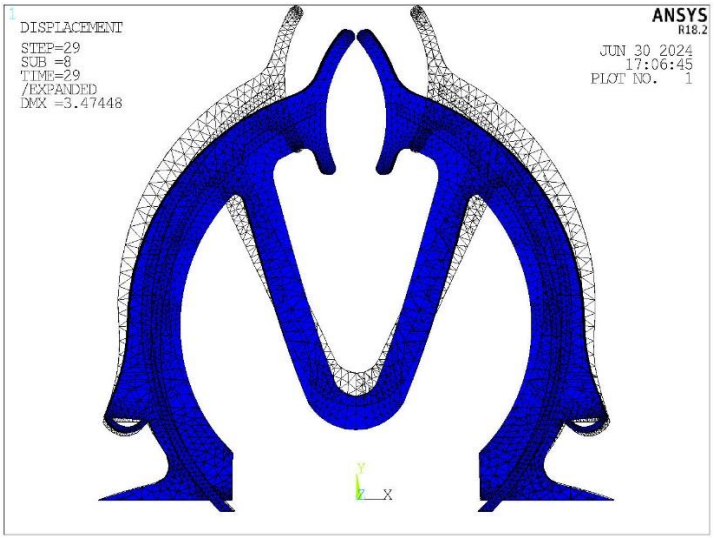

Fig. 5 Deformed shape of the gripper assembly under pressure of 14kPa

throughout the length of the IPMC actuator. Stress and displacement analysis has been done with the application of pressure, 0.01 to 14 KPa, to the actuator. Fig. 5 shows the deformed shape of the gripper assembly under the maximum pressure of 14 KPa in ANSYS R18.2. Figs. 6 and 7 represents the stress distribution of actuator and microgripper assembly respectively. Fig. 8 reveals the distribution of displacement along its length in X-direction. Fig. 9 shows the sum of displacement vector along X and Y direction.

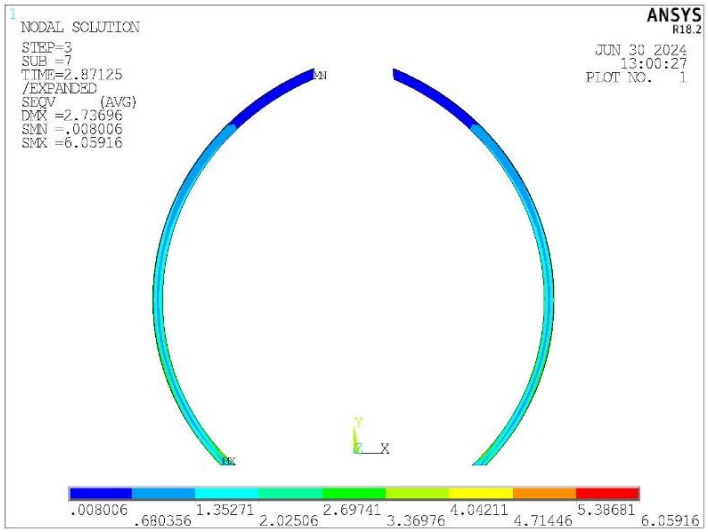

Fig. 6 Stress analysis of IPMC actuator (kPa)

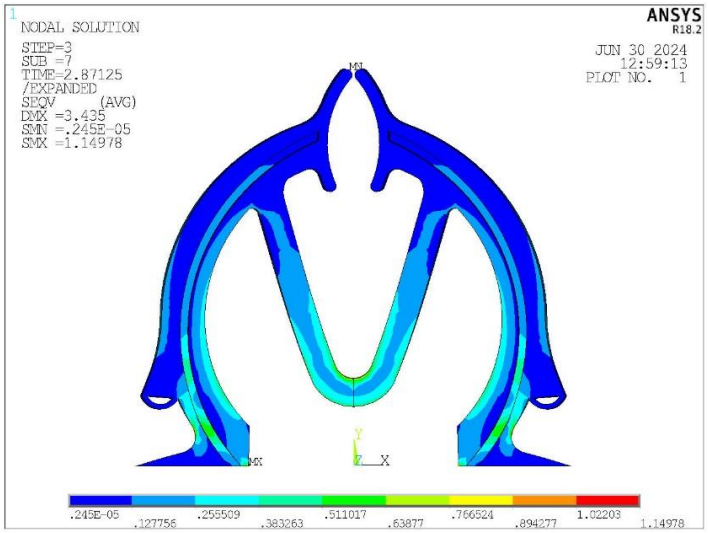

Fig. 7 Stress analysis of TPU microgripper - IPMC actuator assembly (kPa)

4. Finite element analysis of actuator

The actuator, Fig. 2, of the microgripper is subjected to the bending force of 4N corresponding to 0.01MPa of distributed pressure along its surface of dimension $28.77\,mm \times 1\,mm \times 0.81\,mm$ and analysed by finite element method as described by Eqs. (1)-(10).

Co-ordinates can be assumed as

$$\begin{Bmatrix} x \\ y \\ z \end{Bmatrix} = \begin{bmatrix} x_1 & x_2 \cdots & x_8 \\ y_1 & y_2 \ddots & y_8 \\ z_1 & z_2 \cdots & z_8 \end{bmatrix} \begin{Bmatrix} N_1 \\ \vdots \\ N_8 \end{Bmatrix} \tag{1}$$

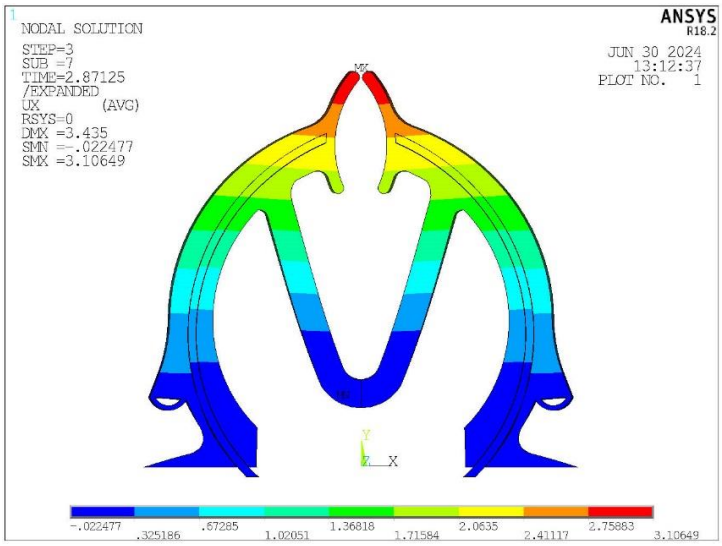

Fig. 8 Displacement analysis of TPU microgripper - IPMC actuator assembly in X-direction (mm)

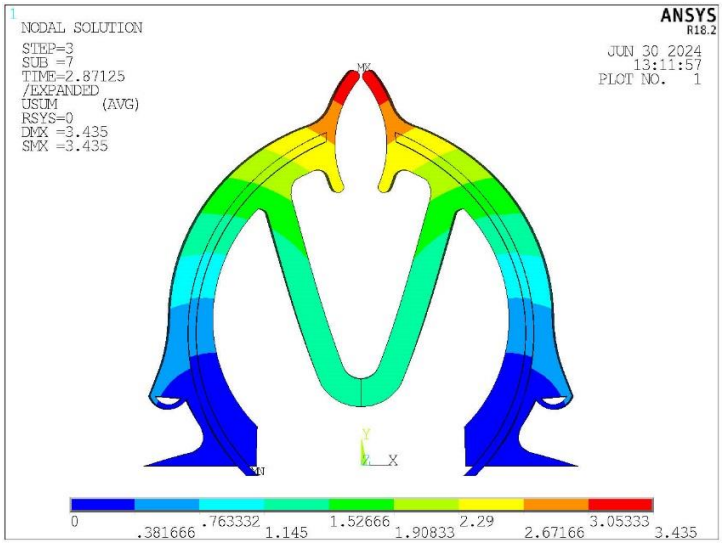

Fig. 9 Displacement vector sum of TPU microgripper - IPMC actuator assembly (mm)

Shape function can be assigned as

$$N_i = (1 + \xi\xi_i)(1 + \eta\eta_i)(1 + \zeta\zeta_i) \tag{2}$$

where (ξ_i, η_i, ζ_i) *are the co-ordinates of the* i^{th} *node*

Field variables can be assumed to be

$$\begin{Bmatrix} u \\ v \\ w \end{Bmatrix} = \begin{bmatrix} u_1 & u_2 \cdots & u_8 \\ v_1 & v_2 \ddots & v_8 \\ w_1 & w_2 \cdots & w_8 \end{bmatrix} \begin{Bmatrix} N_1 \\ \vdots \\ N_8 \end{Bmatrix} \tag{3}$$

$$\begin{Bmatrix}\epsilon_x\\ \epsilon_y\\ \epsilon_z\\ \gamma_{xy}\\ \gamma_{yz}\\ \gamma_{zx}\end{Bmatrix} = \begin{bmatrix} \frac{\delta N_1}{\delta x} & 0 & 0 & \frac{\delta N_2}{\delta x} & 0 & 0 & \dots & \frac{\delta N_8}{\delta x} & 0 & 0 \\ 0 & \frac{\delta N_1}{\delta y} & 0 & 0 & \frac{\delta N_2}{\delta y} & 0 & \dots & 0 & \frac{\delta N_8}{\delta y} & 0 \\ 0 & 0 & \frac{\delta N_1}{\delta z} & 0 & 0 & \frac{\delta N_2}{\delta z} & \dots & 0 & 0 & \frac{\delta N_8}{\delta z} \\ \frac{\delta N_1}{\delta y} & \frac{\delta N_1}{\delta x} & 0 & \frac{\delta N_2}{\delta y} & \frac{\delta N_2}{\delta x} & 0 & \dots & \frac{\delta N_8}{\delta y} & \frac{\delta N_8}{\delta x} & 0 \\ 0 & \frac{\delta N_1}{\delta z} & \frac{\delta N_1}{\delta y} & 0 & \frac{\delta N_2}{\delta z} & \frac{\delta N_2}{\delta y} & \dots & 0 & \frac{\delta N_8}{\delta z} & \frac{\delta N_8}{\delta y} \\ \frac{\delta N_1}{\delta z} & 0 & \frac{\delta N_1}{\delta x} & \frac{\delta N_2}{\delta z} & 0 & \frac{\delta N_2}{\delta x} & \dots & \frac{\delta N_8}{\delta z} & 0 & \frac{\delta N_8}{\delta x} \end{bmatrix} \begin{bmatrix} u_1\\ v_1\\ w_1\\ u_2\\ v_2\\ w_2\\ \vdots\\ \vdots\\ \vdots\\ u_8\\ v_8\\ w_8 \end{bmatrix} \tag{4}$$

$$\{\varepsilon\}_{6X1} = [B]_{6X24}\{d\}_{24X1} \tag{5}$$

From shape function, for all $N_i,\ i = 1\ to\ 8$ in general;

$$\begin{bmatrix}\frac{\delta N_i}{\delta x}\\ \frac{\delta N_i}{\delta y}\\ \frac{\delta N_i}{\delta z}\end{bmatrix} = \begin{bmatrix}\frac{\delta \xi}{\delta x} & \frac{\delta \eta}{\delta x} & \frac{\delta \zeta}{\delta x}\\ \frac{\delta \xi}{\delta y} & \frac{\delta \eta}{\delta y} & \frac{\delta \zeta}{\delta y}\\ \frac{\delta \xi}{\delta z} & \frac{\delta \eta}{\delta z} & \frac{\delta \zeta}{\delta z}\end{bmatrix}\begin{bmatrix}\frac{\delta N_i}{\delta \xi}\\ \frac{\delta N_i}{\delta \eta}\\ \frac{\delta N_i}{\delta \zeta}\end{bmatrix} = [J]^{-1}\begin{bmatrix}\frac{\delta N_i}{\delta \xi}\\ \frac{\delta N_i}{\delta \eta}\\ \frac{\delta N_i}{\delta \zeta}\end{bmatrix} \tag{6}$$

Call [J] as Jacobian, where

$$[J] = \begin{bmatrix}\frac{\delta x}{\delta \xi} & \frac{\delta y}{\delta \xi} & \frac{\delta z}{\delta \xi}\\ \frac{\delta x}{\delta \eta} & \frac{\delta y}{\delta \eta} & \frac{\delta z}{\delta \eta}\\ \frac{\delta x}{\delta \zeta} & \frac{\delta y}{\delta \zeta} & \frac{\delta z}{\delta \zeta}\end{bmatrix} \tag{7}$$

The Real co-ordinates or physical co-ordinates can be expressed as $x_1, x_2, x_3, \dots x_8$; $y_1, y_2, y_3, \dots y_8$; $z_1, z_2, z_3, \dots z_8$

Where Gauss points are

$$(\xi_1, \eta_1, \zeta_1) = \left(-\frac{1}{\sqrt{3}}, -\frac{1}{\sqrt{3}}, -\frac{1}{\sqrt{3}}\right)$$

$$(\xi_2, \eta_2, \zeta_2) = \left(+\frac{1}{\sqrt{3}}, -\frac{1}{\sqrt{3}}, -\frac{1}{\sqrt{3}}\right)$$

$$(\xi_3, \eta_3, \zeta_3) = \left(+\frac{1}{\sqrt{3}}, +\frac{1}{\sqrt{3}}, -\frac{1}{\sqrt{3}}\right)$$

$$(\xi_4, \eta_4, \zeta_4) = \left(-\frac{1}{\sqrt{3}}, +\frac{1}{\sqrt{3}}, -\frac{1}{\sqrt{3}}\right)$$

$$(\xi_5, \eta_5, \zeta_5) = \left(-\frac{1}{\sqrt{3}}, -\frac{1}{\sqrt{3}}, +\frac{1}{\sqrt{3}}\right)$$
$$(\xi_6, \eta_6, \zeta_6) = \left(+\frac{1}{\sqrt{3}}, -\frac{1}{\sqrt{3}}, +\frac{1}{\sqrt{3}}\right)$$
$$(\xi_7, \eta_7, \zeta_7) = \left(+\frac{1}{\sqrt{3}}, +\frac{1}{\sqrt{3}}, +\frac{1}{\sqrt{3}}\right)$$
$$(\xi_8, \eta_8, \zeta_8) = \left(-\frac{1}{\sqrt{3}}, +\frac{1}{\sqrt{3}}, +\frac{1}{\sqrt{3}}\right)$$

Therefor local matrix $[K]_{24X24}$ can be written as

$$[K]_{24X24} = \sum_{\substack{for\ all \\ 8\ guass\ points}} [B]^T_{24X6}\,[D]_{6X6}[B]_{6X24}|J| \tag{8}$$

$$[D] = \frac{E}{(1+\nu)(1-2\nu)}\begin{bmatrix} 1-\nu & \nu & \nu & 0 & 0 & 0 \\ \nu & 1-\nu & \nu & 0 & 0 & 0 \\ \nu & \nu & 1-\nu & 0 & 0 & 0 \\ 0 & 0 & 0 & \frac{1-2\nu}{2} & 0 & 0 \\ 0 & 0 & 0 & 0 & \frac{1-2\nu}{2} & 0 \\ 0 & 0 & 0 & 0 & 0 & \frac{1-2\nu}{2} \end{bmatrix}_{6X6} \tag{9}$$

where $[D]$ is material property

$$[B] = \begin{bmatrix} \frac{\delta N_1}{\delta x} & 0 & 0 & \frac{\delta N_2}{\delta x} & 0 & 0 & \dots & \frac{\delta N_8}{\delta x} & 0 & 0 \\ 0 & \frac{\delta N_1}{\delta y} & 0 & 0 & \frac{\delta N_2}{\delta y} & 0 & \dots & 0 & \frac{\delta N_8}{\delta y} & 0 \\ 0 & 0 & \frac{\delta N_1}{\delta z} & 0 & 0 & \frac{\delta N_2}{\delta z} & \dots & 0 & 0 & \frac{\delta N_8}{\delta z} \\ \frac{\delta N_1}{\delta y} & \frac{\delta N_1}{\delta x} & 0 & \frac{\delta N_2}{\delta y} & \frac{\delta N_2}{\delta x} & 0 & \dots & \frac{\delta N_8}{\delta y} & \frac{\delta N_8}{\delta x} & 0 \\ 0 & \frac{\delta N_1}{\delta z} & \frac{\delta N_1}{\delta y} & 0 & \frac{\delta N_2}{\delta z} & \frac{\delta N_2}{\delta y} & \dots & 0 & \frac{\delta N_8}{\delta z} & \frac{\delta N_8}{\delta y} \\ \frac{\delta N_1}{\delta z} & 0 & \frac{\delta N_1}{\delta x} & \frac{\delta N_2}{\delta z} & 0 & \frac{\delta N_2}{\delta x} & \dots & \frac{\delta N_8}{\delta z} & 0 & \frac{\delta N_8}{\delta x} \end{bmatrix}_{6\times24} \tag{10}$$

5. Static characteristics of IPMC actuator

The actuating link having the dimension of $\mathbf{28.77\ mm \times 1\ mm \times 0.81\ mm}$. Divide it into 500 elements.

We find 500 number of $K_{24\times24}$ matrices $[K_l^i; i = 1\ to\ 500]$ corresponding to each of 500 elements.

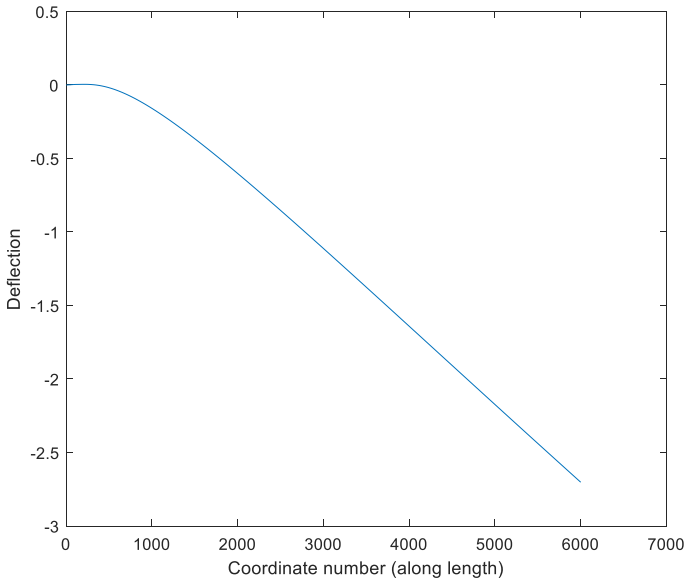

Fig. 10 Bending characteristics of developed IPMC by FEM

As there are 2004 nodes and each node having three degree of freedom $[u, v, w]$, therefore global matrix $\left[K_g\right]_{6012\times6012}$ will be of 6012×6012 and all the local matrix $(K_e)_{i,j}$ will be mapped to global matrix $\left(K_g\right)_{k,l}$. $\{U\}$, the displacement matrix and $\{F\}$, the load matrix can be related by Eqs. (11).

Therefore

$$\left[K_g\right]_{6012\times6012}\{U\}_{6012\times1} = \{F\}_{6012\times1}$$

$$U = \begin{Bmatrix} u_1 \\ v_1 \\ w_1 \\ u_2 \\ v_2 \\ w_2 \\ .. \\ .. \\ u_{2004} \\ v_{2004} \\ w_{2004} \end{Bmatrix}_{6012\times1} \quad ; \quad F = \begin{Bmatrix} F_{1X} \\ F_{1Y} \\ F_{1Z} \\ F_{2X} \\ F_{2Y} \\ F_{2Z} \\ .. \\ .. \\ F_{2004X} \\ F_{2004Y} \\ w_{2004Z} \end{Bmatrix}_{6012\times1} \tag{11}$$

Therefore displacement matrix can be evaluated as Eqs. (12)

$$\{\boldsymbol{U}\} = \left[\boldsymbol{K_g}\right]^{-\mathbf{1}}\{\boldsymbol{F}\} \tag{12}$$

Now load matrix $\{F\} = 4N$

For dimension length= 28.77 mm,

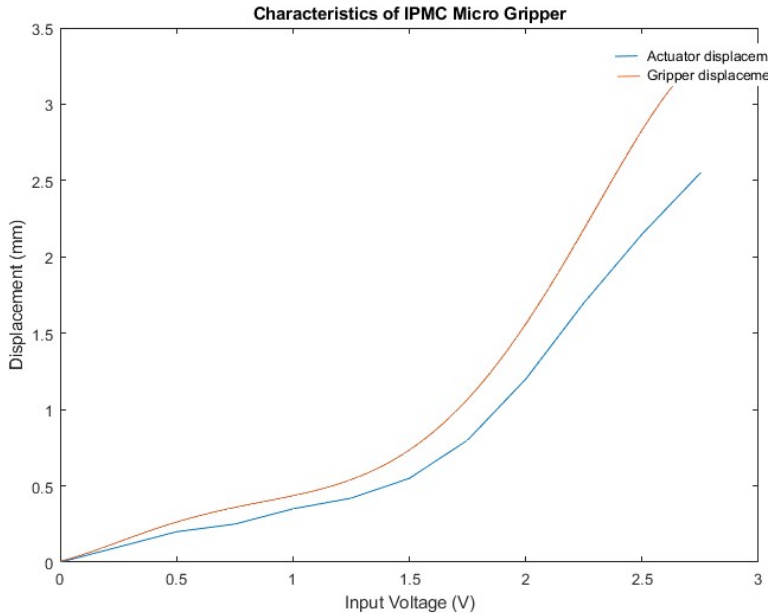

Fig. 11 Input output characteristics of actuator and gripper

Cross section= 1.0 mm X 0.81 mm.

$E = 105\ MPa$

Tensile stress at yield= 21 MPa

$\nu = 0.4$

$L = 28.77\ mm = 28.77 \times 10^{-3} m$

$b = 1.0\ mm = 1.0 \times 10^{-3} m$

$h = 0.81\ mm = 0.81 \times 10^{-3} m$

$A = 0.81 \times 10^{-6} m^2$

$F = 4\ N$

Fig. 10 shows the deflection of IPMC actuator under the nominal load condition along its all coordinates 0 to 6012 by FEM and evaluated as 2.69 mm.

Therefore

$\delta_{Ymax} = 2.69\ mm$

6. System modelling of microgripper system in MATLAB

Input output characteristics of the actuator and the gripper has been obtained by FEA using ANSYS R18.2 and presented in Fig. 11. The characteristic curve is used by System Identification toolbox in MATLAB to model the actuator and microgripper system and shown in Fig. 12. Fig. 13 shows the validation of estimated actuator model with respect to evaluated output. Figs. 14 and 15 presents the microgripper model estimation and corresponding output validation respectively.

$$TF2 = \frac{GD(s)}{AD(s)} = \frac{1.305s + 0.03249}{s + 0.02511} \tag{14}$$

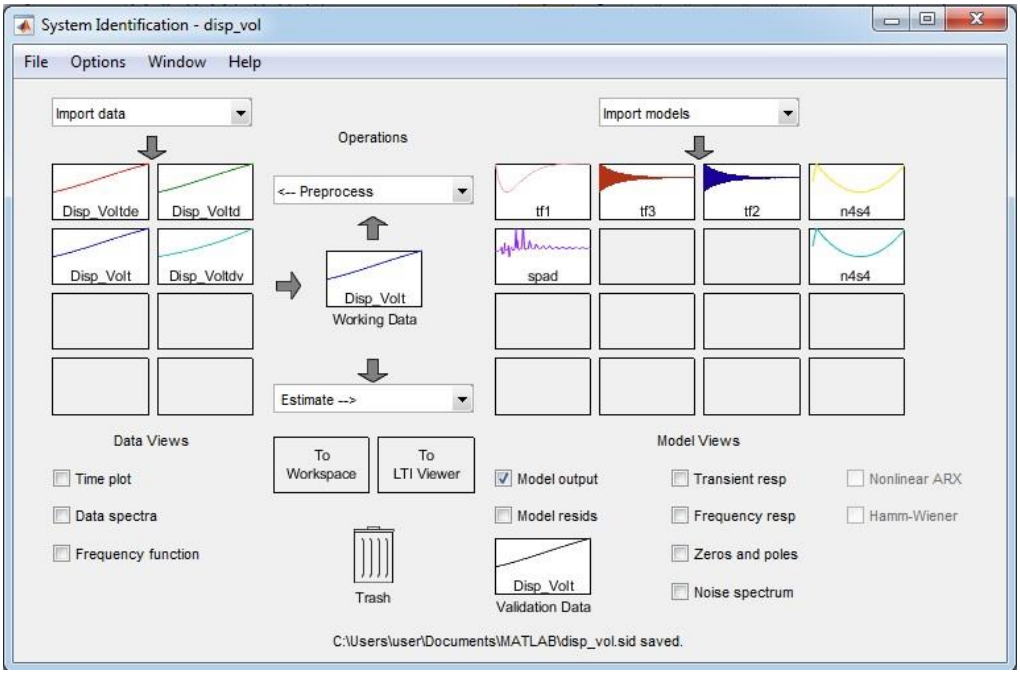

Fig. 12 Parameterization of actuator using System Identification Toolbox in MATLAB

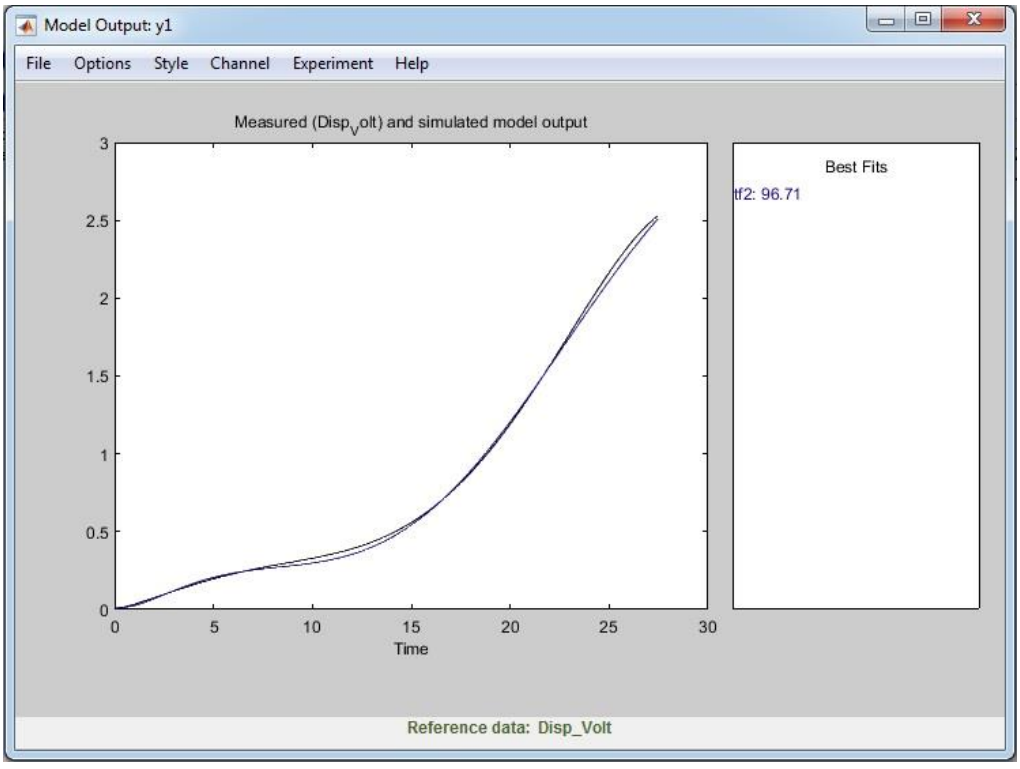

Fig. 13 Validation of actuator model output in System Identification Toolbox in MATLAB

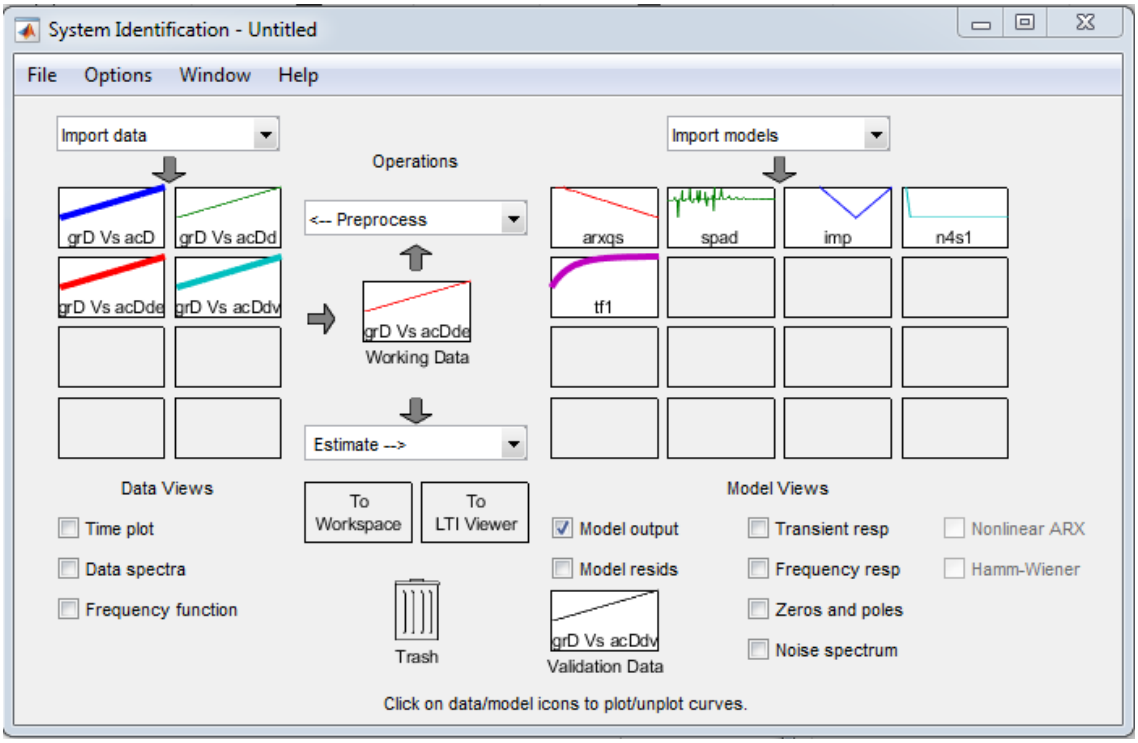

Fig. 14 Parameterization of gripper using System Identification Toolbox in MATLAB

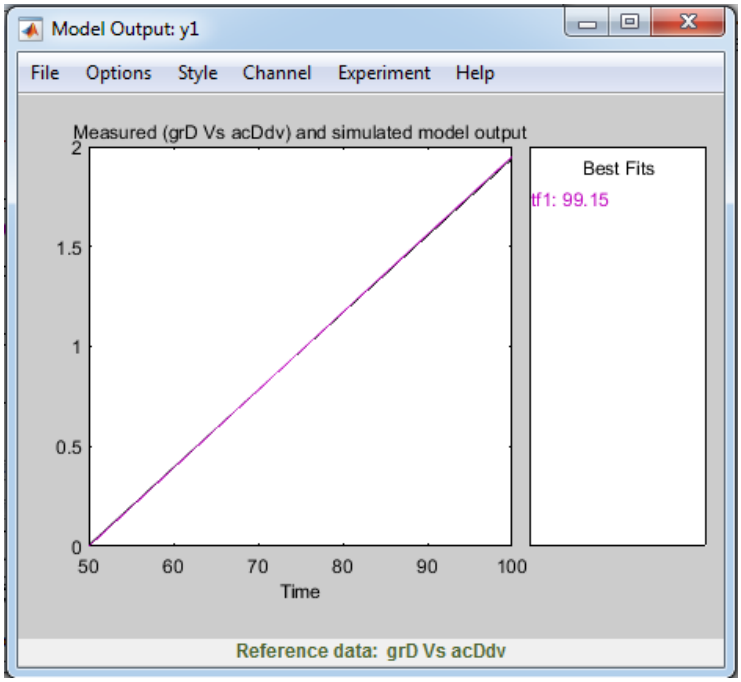

Fig. 15 Validation of gripper model output using System Identification Toolbox in MATLAB

Table 2 Deflection due to applied force of 4 N

	Deflection (mm)	Dimension	Improvement (%)
Standard actuator	2.55	$40\ mm \times 10\ mm \times 0.2\ mm$	5.4
Developed actuator by FEA (number of elements = 500) using MATLAB	2.69	$28.77\ mm \times 1\ mm \times 0.81\ mm$	

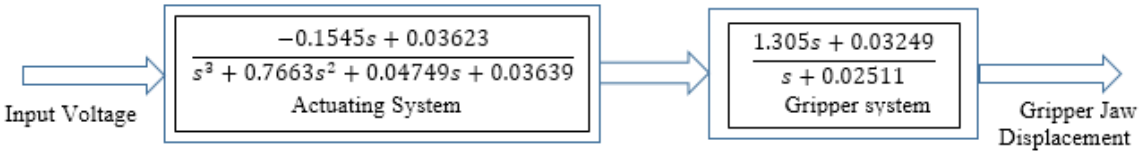

Fig. 16 Block diagram of microgripper system

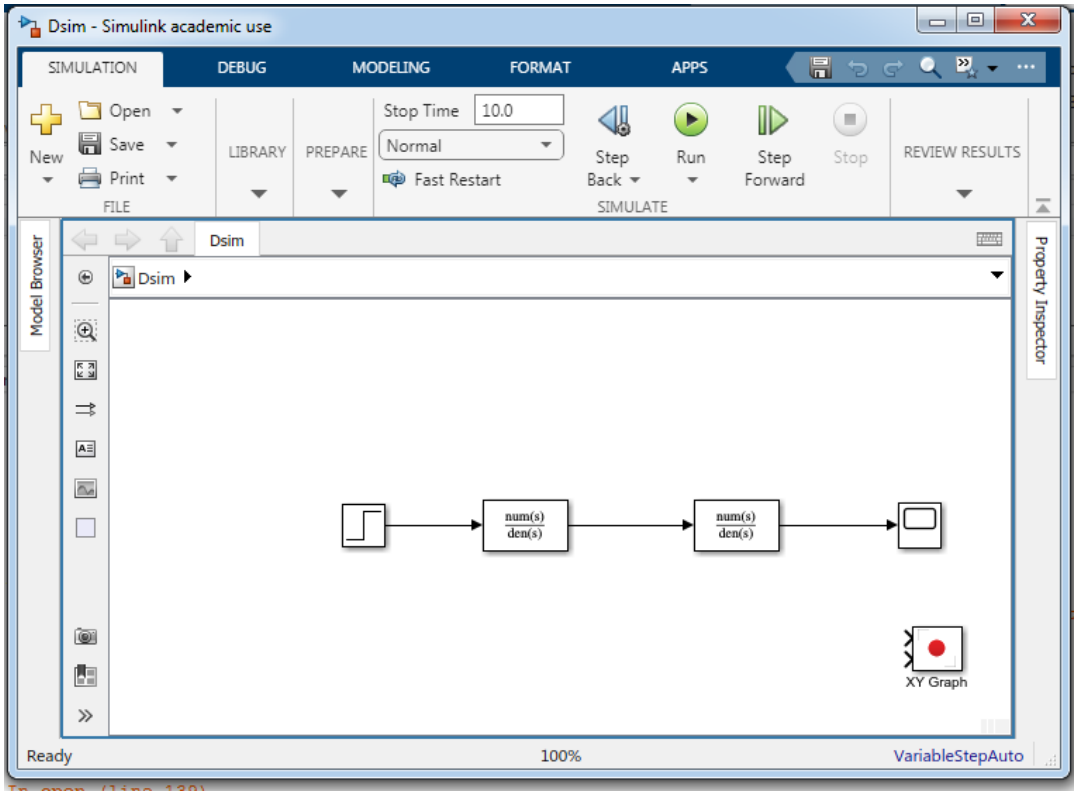

Fig. 17 Simulink Block diagram of microgripper system

Parameterization:
Number of poles: 1 Number of zeros: 1
Number of free coefficients: 3
Fit to estimation data: 99.98% (stability enforced)
FPE: 1.149e-08, MSE: 1.135e-08

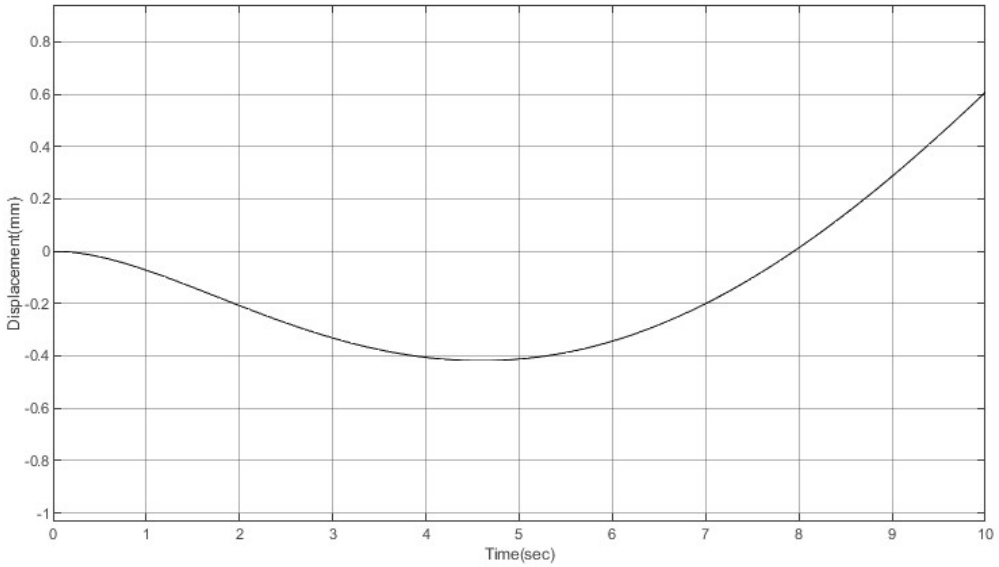

Fig. 18 Simulink result of gripper jaw displacement for 1V step input

7. Results and Discussions

Actuator model and gripper model has been estimated using System Identification Tool box in MATLAB and estimated transfer function models are given in Eqs. (13) and (14) respectively. The estimated model of actuator system has three poles and one zero for output validation of 96.71% goodness of fit with final prediction error (FPE) and mean squared error (MSE) of 0.000638 and 0.0006021 respectively. The microgripper estimated model may be considered as the linear displacement amplifier with 99.98% goodness of fit and FPE and MSE of 1.149e-08 and 1.135e-08 respectively. The deflection of the designed actuator gives 5.4% improvement over standard one as given in Table II. Figs. 16 and 17 show the block diagram and Simulink block diagram of microgripper system respectively. The dynamic output of the cascade system for 1V step input voltage is presented in Fig. 18.

8. Conclusions

A compliant microgripper of TPU with smart actuation using IPMC has been designed. The primary objective was to design a compliant microgripper which will be flexible, light weight and strong enough for micromanipulation. This has been achieved by selecting the suitable material TPU which is comparatively more flexible and lightweight to ABS (Acrylonitrile Butadiene Styrene) and PLA (Polylactic Acid). The active component of the microgripper consisting of IPMC, an EAP (Electro active polymer), which is able to be deformed by bending with the application of electrical energy. This deformation is used as the actuating force for the micro-gripper to handle light weight object for micromanipulation. From the results obtained from the above modelling and simulation, it can be assumed that the identified model of the system is capable of producing the desired output as obtained from the characteristic curve.

References

Abderezak, R.A., Daouadji, T.H. and Rabia, B. (2021), "Modeling and analysis of the imperfect FGM-damaged RC hybrid beams", *Adv. Comput. Des.*, **6**(2), 117-133. https://doi.org/10.12989/acd.2021.6.2.117.

Al-Maliki, A.F.H., Ahmed, R.A., Moustafa, N.M. and Faleh, N.M. (2020), "Finite element based modeling and thermal dynamic analysis of functionally graded graphene reinforced beams", *Adv. Comput. Des.*, **5(**2), 177-193. https://doi.org/10.12989/acd.2020.5.2.177.

Ali, H.A.K., Al-Toki, M.H.Z., Fenjan, R.M. and Faleh, N.M. (2022), "Nonlinear static analysis of smart beams under transverse loads and thermal-electrical environments", *Adv. Comput. Des.*, **7(**2), 99-112. https://doi.org/10.12989/acd.2022.7.2.099.

Bagchi, A., Biswas, A., Singh, G., Sarkar, S. and Mukhopadhyay, P.K. (2021), "Finite element analysis of a FSMA microgripper for determination of force experienced by it due to photo induced micro actuation effect", *J. Micro Bio Robot*, **17**(2), 79-92. https://doi.org/10.1007/s12213-022-00147-0.

Benhenni, M.A., Daouadji, T.H., Abbes, B., Adim, B., Li, Y. and Abbes, F. (2018), "Dynamic analysis for anti-symmetric cross-ply and angle-ply laminates for simply supported thick hybrid rectangular plates", *Adv. Mater. Res.*, **7**(2), 83-103. https://doi.org/10.12989/amr.2018.7.2.119.

Biswal, D.K., Bandopadhya, D. and Dwivedy, S.K. (2014), "Dynamic modeling and effect of dehydration on segmented IPMC actuators following variable parameter pseudo-rigid body modeling technique", *Mech. Adv. Mater. Struct.*, **21**(2), 129-138. https://doi.org/10.1080/15376494.2012.680665.

Daouadji, T.H., Rabahi, A., Abbes, B. and Adim, B. (2016), "Theoretical and finite element studies of interfacial stresses in reinforced concrete beams strengthened by externally FRP laminates plate", *J. Adhesion Sci. Technol.*, **30**(12), 1253-1280. https://doi.org/10.1080/01694243.2016.1140703.

Ertas, A.H. and Sonmez, F.O. (2011), "Design optimization of composite structures for maximum strength using direct simulated annealing", *P. I. Mech. Eng. C-J. Mec*, **225**(1), 28-39. https://doi.org/10.1243/09544062JMES2105.

Gupta, A. and Mukherjee S. (2022), "Actuation characteristics and experimental identification of IPMC actuator for underwater biomimetic robotic application", *Mater. Today Proc.*, **62**, 7461-7466. https://doi.org/10.1016/j.matpr.2022.03.388.

Hassan, A. and Abomoharam, M. (2017), "Modeling and design optimization of a robot gripper mechanism", *Robot. Comput. Integr. Manuf.*, **46**, 94-103. https://doi.org/10.1016/j.rcim.2016.12.012.

Kang, L., Kim, S. and Yi, B. (2021), "Modeling, design, and implementation of an underactuated gripper with capability of grasping thin objects", *Machines*, **9**(12), 347-373. https://doi.org/10.3390/machines9120347.

Karpik, A., Cosco, F. and Mundo, D. (2023), "Higher-order hexahedral finite elements for structural dynamics: a comparative review", *Machines*, **11**(3), 326-349. https://doi.org/10.3390/machines11030326.

Kayikci, R. and Sonmez, F.O. (2012), "Design of composite laminates for optimum frequency response", *J. Sound Vib.*, **331**(8), 1759-1776. https://doi.org/10.1016/j.jsv.2011.12.020.

Mandal, R.R. and Dewangan, U.K. (2017), "Finite element modeling of beam with eight noded brick element using Matlab", *Int. J. Civil Eng. Technol.*, **8**(5), 646-656.

Pavarino, E., Neves, L.A., Machado, J.M., de Godoy, M.F., Shiyou, Y., Momente, J.C., Zafalon, G.F., Pinto, A.R. and Valêncio, C.R. (2013), "Tools and strategies for the generation of 3D finite element meshes: Modeling of the cardiac structures", *Int. J. Biomed. Imag.*, **2013**(1), 540571. https://doi.org/10.1155/2013/540571.

Polatov, A.M., Ikramov, A.M. and Razmukhamedov, D.D. (2020), "Finite element modeling of multiply-connected three-dimensional areas", *Adv. Comput. Des.*, **5**(3), 277-289. https://doi.org/10.12989/acd.2020.5.3.277.

Ramasubramanian, A.K., Connolly, M., Mathew, R. and Papakostas, N. (2022), "Automatic simulation-based design and validation of robotic gripper fingers", *CIRP Annals Manuf. Technol.*, **71**(1), 137-140. https://doi.org/10.1016/j.cirp.2022.04.054.

Shan, Y., Zhao, Y., Yu, H., Pei, C., Jin, Z. and Sun, Y. (2023), "Design and grasping force modeling for a soft robotic gripper with multi-stem twining", *J. Bio. Eng.*, **20**(5), 2123-2134. https://doi.org/10.1007/s42235-023-00371-9.

Sun, A.B., Bajon, D., Moschetta, J., Benard, E. and Thipyopas, C. (2014), "Integrated static and dynamic modeling of an ionic polymer–metal composite actuator", *J. Intell. Mater. Syst. Struct.*, **26**(10), 1164-1178. https://doi.org/10.1177/1045389X14538528.

Tariq, M.O., Ahmed, J. and Bazaz, S.A. (2022), "Analytical design and finite element analysis of a microgripper for characterizing a single microcapsule", *Meas. Sci. Technol.*, **34**(1), 15118. https://doi.org/10.1088/1361-6501/ac9495.

Vokoun, D., He, Q., Heller, L., Yu M. and Dai, Z. (2015), "Modeling of ipmc cantilever's displacements and blocking forces", *J. Bio. Eng.*, **12**(1), 142-151. https://doi.org/10.1016/S1672-6529(14)60108-6.

Yang, Y., Wu, G. and Wei Y. (2021), "Design, modeling, and control of a monolithic compliant x-y-θ microstage using a double-rocker mechanism", *Precis. Eng.*, **71**(6), 209-231. https://doi.org/10.1016/j.precisioneng.2021.03.014.

You, Y., Sun, M. and Lee, Y. (2021), "Design and analysis of offshore wind structure", *Adv. Comput. Des.*, **8(**3), 191-217. https://doi.org/10.12989/acd.2023.8.3.191.

Zhao, Y., Huang, X., Liu, Y., Wang, G. and K. Hong (2020), "Design and control of a piezoelectric-driven microgripper perceiving displacement and gripping force", *Micromachines*, **11**(2), 121-132. https://doi.org/10.3390/mi11020121.

CC